Effects of permeability and compressibility on liquefaction screening using cone penetration resistance

S. Thevanayagam and N. Ecemis

University at Buffalo, State University of New York, Buffalo, NY 14260, USA

ABSTRACT:

Sands and silty sands with the same liquefaction resistance can have significantly different hydraulic conductivity and coefficient of consolidation. Numerical simulations of cone penetration resistance taking into account the effects of silt content and consolidation characteristics show that the penetration resistances are significantly affected by consolidation characteristics for sands and silty sands with similar liquefaction resistances. The influence of permeability and consolidation characteristics on pore pressures around the cone tip and cone penetration resistances are presented. Relationships between liquefaction resistance, cone penetration resistance, and a normalized penetration rate ($T=vd/c_h$) are presented and compared with current field-based CPT-liquefaction screening methods. The proposed relationships are compared with the experimental results obtained from a limited number of full-scale 1-g laminar box shake table liquefaction experiments and cone penetration tests.

1 INTRODUCTION

Current liquefaction screening techniques rely on knowledge from extensive laboratory research conducted on liquefaction resistance of clean sands, and extrapolations of observed field performance during past earthquakes (NCEER 1997). Such observations have been documented in the form of normalized penetration resistance (SPT $(N_1)_{60}$, CPT q_{c1N}) (Seed et al. 1983, Robertson and Wride 1997), and shear wave velocity (v_{s1}) (Andrus and Stokoe, 2000) versus cyclic stress ratio (CSR) induced by the earthquakes, corrected for magnitude, for many sites where occurrence or non-occurrence of liquefaction were recorded during the earthquakes. A liquefaction-screening chart based on CPT resistance is shown in Figs.1a-b. Cyclic resistance ratio (CRR), applicable for a standard earthquake magnitude of 7.5, of a soil deposit with a known value of q_{c1N} is obtained from a demarcation line drawn between the field-observation-based data points which correspond to liquefied sites and those that did not liquefy in Fig.1a. This is denoted as $CRR_{7.5}$. This CRR is compared against the anticipated cyclic stress ratio (CSR) for that deposit due to a design earthquake of the same magnitude to determine whether or not that deposit would liquefy. Factor of safety (FS) against liquefaction is defined as $FS=CRR_{7.5}/CSR$. If a different design earthquake magnitude is expected, the $CRR_{7.5}$ is multiplied by a magnitude scaling factor (MSF) to account for the differences in number of cycles, frequency content, etc. ($FS= MSF*CRR_{7.5}/CSR$). Researchers have observed that the CRR determined in this manner depends on silt content of the soil for a given q_{c1N}. While this practice has been successful, a rational understanding of this procedure has been lagging. Successful application of this procedure to other sites require an understanding of the phenomenon observed, its limitations, and possible modifications required for it to be applied successfully for a different site, where necessary.

This has sparked numerous researches on the effects of silt on cyclic resistance of silty sands (e.g.Vaid 1994, Koester 1994, Zlatovic and Ishihara 1997) and its effects on liquefaction screening (e.g. Carraro et al. 2003). Recently it has been shown that silt content affects permeability, compressibility, and consolidation characteristics of silty sands and therefore influences the penetration resistance. Two soils with the same cyclic resistance may have different silt contents and different coefficients of consolidation. Their cone resistance would be different due to partial drainage which occurs around the cone and therefore would be expected to show different penetration resistances. A unique

correlation between cyclic resistance and penetration resistance is not possible without considering the effects of coefficient of consolidation on penetration resistance (Thevanayagam et al. 2003, Thevanayagam and Martin 2002,). The authors' previous work focused on the numerical simulation of the effects of consolidation characteristics of silty sands on cone penetration resistance and a possible correlation between the cyclic resistance, cone penetration resistance and a non-dimensional parameter T (vd/c_h) (Thevanayagam et al. 2006) where v=penetration rate, d=cone diameter, and c_h=coefficient of consolidation. The numerical simulations reported in that study ignored the effect of dilation angle. Dilation angle was assumed to be zero. This paper focuses on the effects of compressibility and consolidation characteristics of silty sands on cone penetration resistance with due consideration of the effects of dilation angle on cone penetration resistance. A revised liquefaction-screening chart that takes into account the effects of consolidation characteristics on penetration resistance is presented.

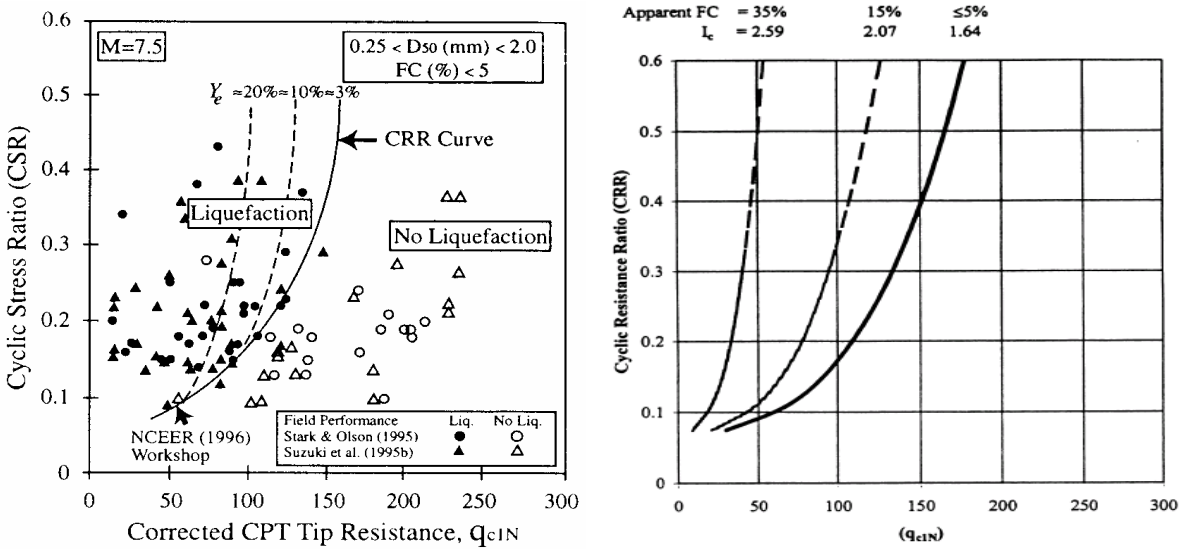

Fig.1 Field Liquefaction Screening Charts using CPT
(Youd and Gilstrap 1999, Stokoe et al. 1999)

2 CONE PENETRATION RESISTANCE

2.1 Finite Element Model

In order to study the effect of permeability and compressibility and the associated partial drainage conditions around the cone tip on cone penetration resistance of sand and silty soils a numerical simulation study was conducted using finite element code ABAQUS (2000). During penetration of the cone, cavity expansion occurs, the stress fields around the cone changes, excess pore pressures are induced, and fluid flow and consolidation occur. These aspects of the problem can be treated in ABAQUS. The soil around the cone penetrometer was simulated using Drucker-Prager model. An axis-symmetric model of a cone and the surrounding soil with the finite element mesh used in the analysis is given in Fig.2. The diameter d of the cone is 4.37 cm, and the cone is placed to a depth of 36 cm from the top surface of the finite element mesh. The mesh extends to a distance of 54 cm (about 15 d) below the cone tip. The mesh also extends horizontally to a distance of 40 cm away from the cone axis. This is about 18 times the radius of the cone. A vertical effective stress of 100 kPa is imposed at the top surface of the mesh to simulate the cone at a depth with about 100 kPa effective vertical stress.

Soil is modelled using elements with eight displacement nodes, whereas elements with four displacement nodes are used to model the cone. Axis-symmetric elements are used since both the geometry of the model and loadings are axis-symmetric. To alleviate stress concentration problems at a sharp cone tip, it was assumed that the cone has a rounded tip. Aubeny (1992) has shown that this approximation has minimal influence on the prediction of pore pressure response near the cone. The mesh close to the cone tip is more congested with elements so that the variation of response around the

cone could be monitored with higher accuracy. The points in the soil located along the axis of symmetry of the cone do not experience any horizontal displacements. In order to bypass this difficulty, the points located on the axis of symmetry were removed from the finite element mesh and a tiny hole was introduced around the axis of symmetry. The soil is fully saturated. Fig. 2 also shows the boundary conditions used in the finite element model for a site having uniform soil. On the bottom and two vertical sides, the normal component of displacement and fluid flow are fixed at zero. No pore fluid flow is permitted across cone body.

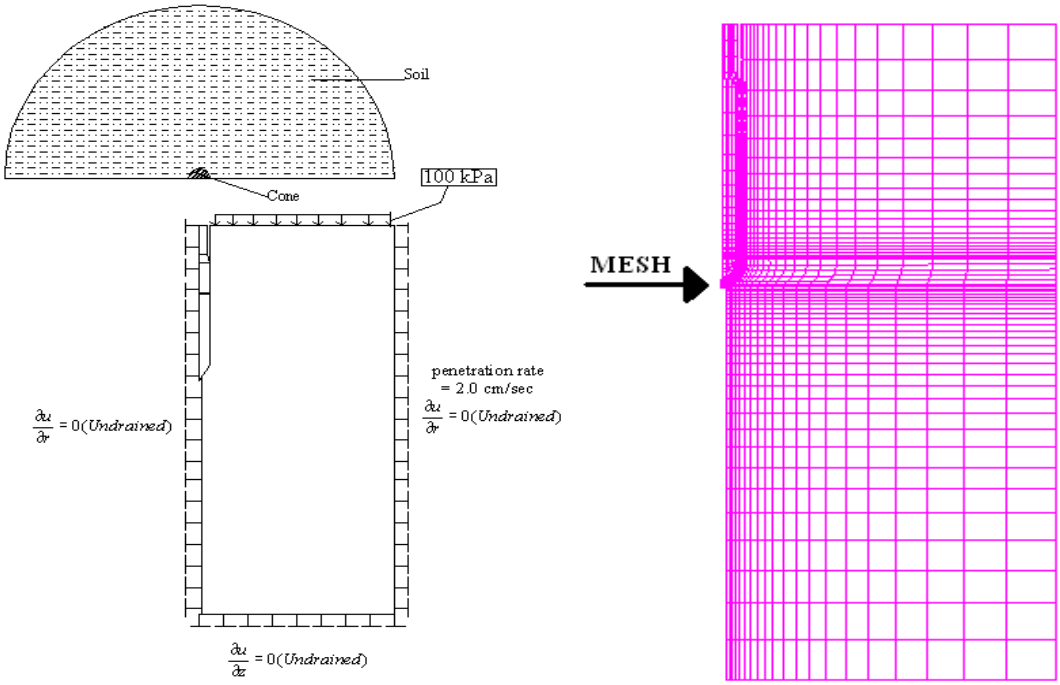

Fig. 2 Finite element mesh – CPT model

A step-by-step time-series analysis is required to obtain solutions for pore pressures and penetration resistances. ABAQUS uses a tolerance on the maximum change in pore pressure allowed in increment to control the time stepping. This, and all other such tolerances, can be controlled. In nonlinear analysis the total load applied in a step is broken into smaller increments so that the nonlinear solution path can be followed.

2.2 **Effect of permeability and compressibility on excess pore pressure and normalized cone tip resistance**

Several sets of cone penetration simulations were made using ABAQUS. As a first step, material properties required for numerical simulation of cone penetration were obtained from several sets of triaxial test data on Ottawa sand and sand-silt mixes (Thevanayagam et al. 2003). Each of the triaxial tests was simulated using ABAQUS and compared with actual triaxial test data to assess the effectiveness of ABAQUS to model soil behaviour (Ecemis, 2007). A typical comparison of stress-strain curve is shown in Fig.3. The dilation angle versus equivalent relative density, $(D_{rc})_{eq}$ obtained from the experimental data combined with comparisons with ABAQUS simulation of the triaxial test data is shown in Fig.4. Equivalent relative density $(D_{rc})_{eq}$ has been found to be a unifying parameter to characterize sands and silty sands in a unified framework (Thevanayagam et al., 2003).

Next, several cone penetration simulations were done for each of the soils at different equivalent relative densities for which soil parameters were available. Pore pressure responses and cone penetration resistances were monitored with penetration of the cone at a constant penetration speed of v = 2 cm/s (ASTM standard) until a steady state was reached. Following this, these simulations were repeated for the same soil parameters for each soil, but at different hydraulic conductivities to study the effect of permeability on cone resistance. The pore pressure at the tip of the cone was plotted against a normalized penetration rate ($T=vd/c_h$) and equivalent relative density $(D_{rc})_{eq}$ (Fig.5a). Note

that the c_h values applicable for pore pressure dissipation during cone penetration are those applicable for over-consolidated soils (Baligh and Levadoux, 1996). The normalized cone resistance q_{c1N} was also plotted against T and $(D_{rc})_{eq}$ (Fig.5b). The q_{c1N} values for a given $(D_{rc})_{eq}$ depends on T. It has been shown before that a sand and silty sand at the same $(D_{rc})_{eq}$ show nearly the same liquefaction resistance irrespective of silt content or permeability of the soil (Thevanayagam et al. 2002, 2003 and Thevanayagam 2007). This indicates a possible relationship between q_{c1N}, cyclic resistance, and T.

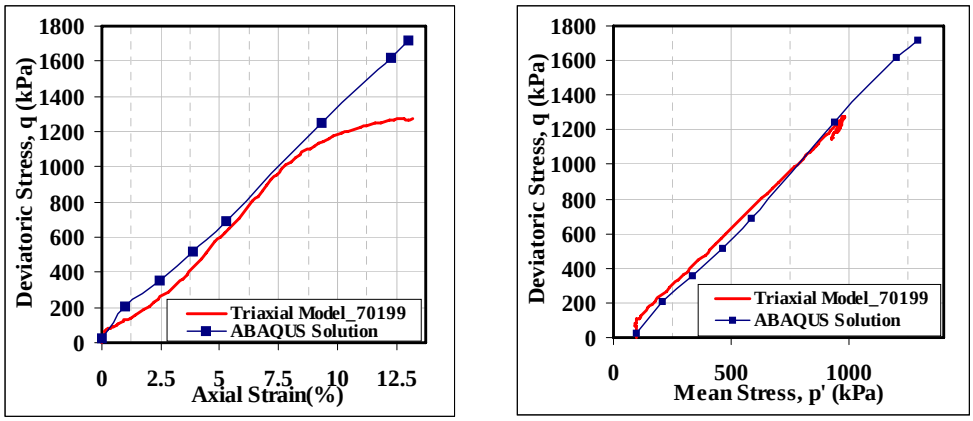

Fig. 3 Typical ABAQUS Simulation Results versus Triaxial Test Data ($(D_{rc})_{eq}$=63%)

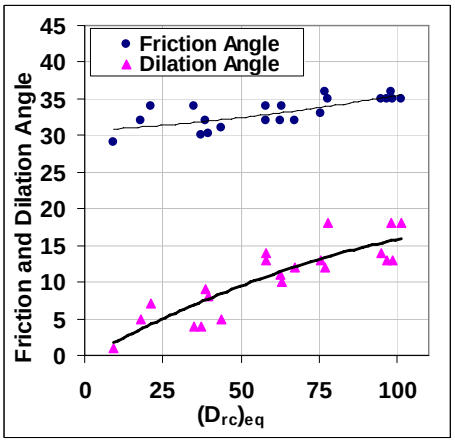

Fig.4 Friction and Dilation Angle vs. $(D_{rc})_{eq}$

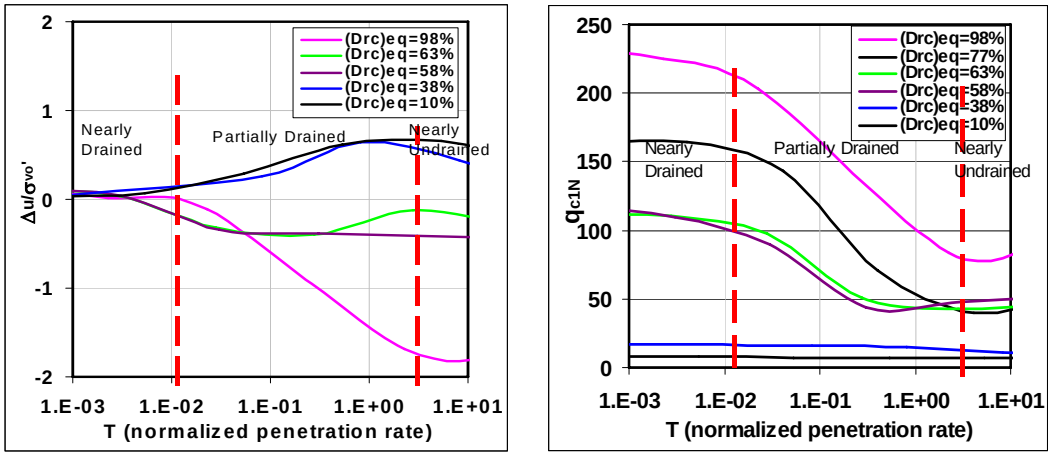

(a) Excess Pore pressure (b) Normalized cone resistance

Fig. 5 Excess pore pressure and normalized cone tip resistance

2.2.1 *Excess pore pressure and normalized cone tip resistance*

Figs.5 (a)-(b) show typical results of normalized excess pore water pressure and normalized cone tip resistance response for a few of the simulations, respectively. For loose soils, the excess pore pressure at the cone tip steadily increases with an increase in T as shown in Fig.5 (a). Beyond a value of T in the range of about 5 to 10, the excess pore pressure ratio reaches a high value and remains little affected by further increase in T, indicating nearly undrained penetration. Similarly at values of T less than about 0.05 to 0.01 the excess pore pressure is small and is little affected by further decrease in T, indicating a highly drained condition around the probe. A partially drained condition prevails at intermediate T values of about 5 to 0.01. In the case of dense soils, the excess pore pressure is small for T values less than about 0.05 to 0.01, indicating drained soil response during cone penetration. At high values of T in the range of about 5 to 10, the excess pore pressure is negative and remains unaffected by further increase in T. This is indicative of highly dilative response of the soil and undrained conditions around the cone. For intermediate values of T, the excess pore pressure is affected by T, indicating existence of partial drainage effects around the cone tip. These effects are reflected in the normalized cone penetration resistance in Fig.5.b. In the analysis, the tip force is calculated through the integration of vertical and shearing stresses at elements in contact with the cone. The tip force is then divided by cone area to obtain the tip resistance.

Figs. 6(a)-(c) show the excess pore water pressures around the cone tip for a loose and medium sand soil at $(D_{rc})_{eq}$=45%, and 58%, respectively, for three different permeabilities, k=10^{-3}, 10^{-5}, and 10^{-7} m/sec, respectively. The pore water pressures are shown in N/cm^2. For the loose soil, the excess pore water pressures at the cone tip are negligibly small (less than 4.2kPa) for T =3x10^{-4} (k=10^{-3}m/sec), whereas the pore water pressure was very high for T=3 (k=10^{-7}m/sec) (more than 75kPa). For intermediate value of T=3x10^{-2} (k=10^{-5}m/sec), an intermediate pore water pressure of 24kPa is observed. Small pore water pressures are indicative of nearly fully drained soil response near the cone tip during penetration. High pore water pressures for T=3, shows a nearly undrained soil response. The corresponding q_{c1N} values are 26 for T=3x10^{-4}, 24 for T=3x10^{-2}, and 23 for T=3. For loose soils there is a slight decrease in q_{c1N} with increase in T.

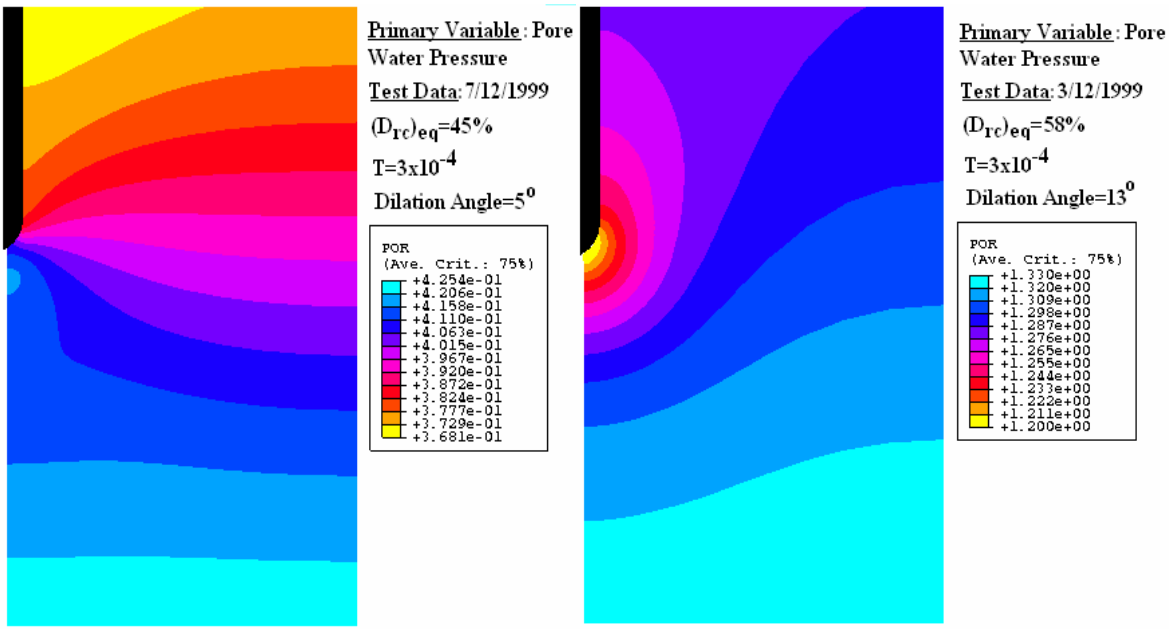

(i) $(D_{rc})_{eq}$=45% (ii) $(D_{rc})_{eq}$=58%

(a) T=3x10^{-4} (Nearly Drained Condition, k=10^{-3} m/sec)
Fig.6 Excess Pore Pressure Response at cone tip

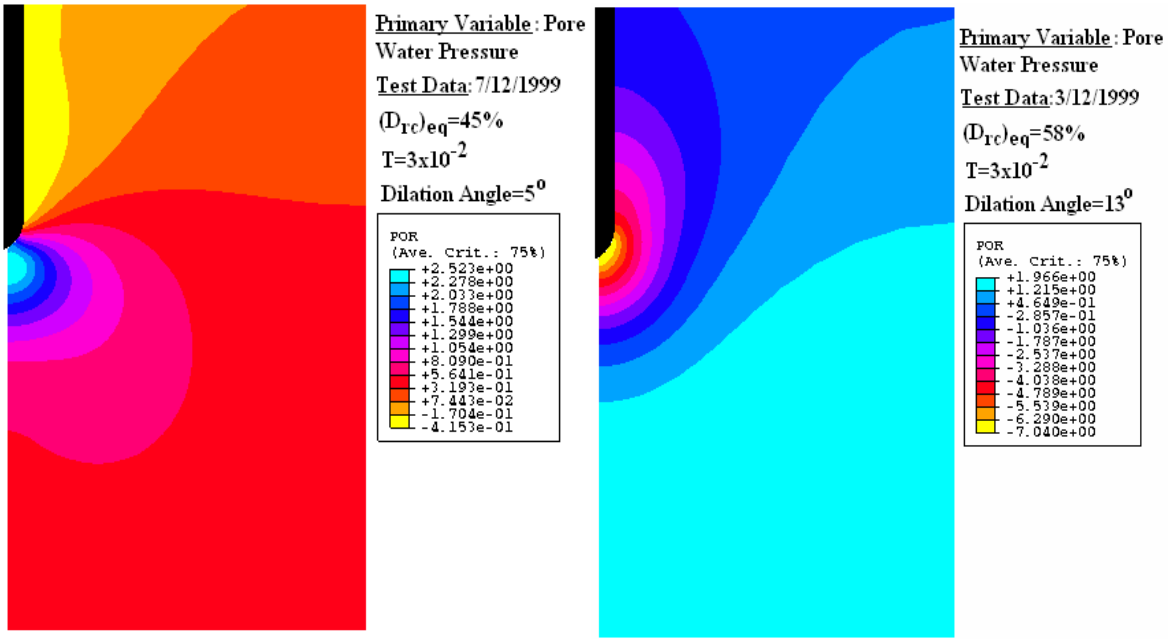

(i) $(D_{rc})_{eq}$=45% (ii) $(D_{rc})_{eg}$=58%

(b) T=3x10^{-2} (Partially Drained Condition, k=10^{-5} m/sec)

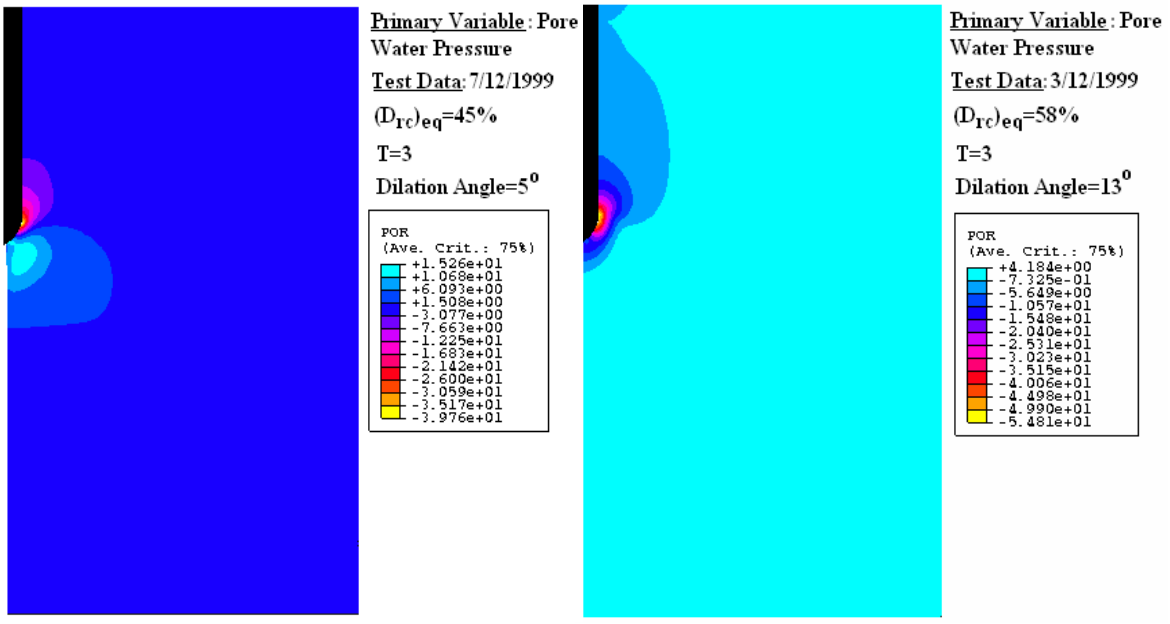

(i) $(D_{rc})_{eq}$=45% (ii) $(D_{rc})_{eq}$=58%

(c) T=3 (Nearly Undrained Condition, k=10^{-7} m/sec)

Fig.6 Excess Pore Pressure Response at cone tip (cont'd)

For the dense soil at $(D_{rc})_{eq}$=58% the excess pore pressure at the cone tip are 11.4kPa for T=3x10^{-4}, -35kPa for T=3x10^{-2}, and - 41kPa for T=3. The corresponding q_{c1N} values are 117 for T=3x10^{-4}, 90 for T=3x10^{-2}, and 48 for T=3. For a medium dense soil there is a significant decrease in q_{c1N} with increase in T. The effect of permeability on q_{c1N} is high for medium-dense soils in contrast with a loose soil.

Observations shown in Fig.6 imply that, for the same equivalent relative density, q_{c1N} for a low permeable silty soil would be smaller than that of highly permeable clean sand at the same $(D_{rc})_{eq}$. This difference is attributable to the presence of fines, which causes undrained or partially drained conditions during penetration in silty soils leading to a decrease in tip resistance compared to highly permeable sand. Low hydraulic conductivity and high T values for silty soils contribute to a slow rate of dissipation of excess pore pressures in silty sands leading to lower effective stress near the penetration tip of a cone than in clean sand at the same $(D_{rc})_{eq}$. Hence a lower penetration resistance for the silty sand than a sand at the same $(D_{rc})_{eq}$. The effect of permeability is larger at higher densities.

3 LIQUEFACTION RESISTANCE AND PENETRATION RESISTANCE

3.1 CRR versus q_{c1N}

The q_{c1N} values obtained from the above numerical simulations were also plotted against undrained cyclic resistance ratio (CRR) for each soil corresponding to 15 cycles obtained from laboratory undrained cyclic triaxial compression tests (Thevanayagam et al. 2003) corrected for field loading conditions (Castro 1975, Seed et al. 1978) to account for multi-directional shaking and modes of shear.

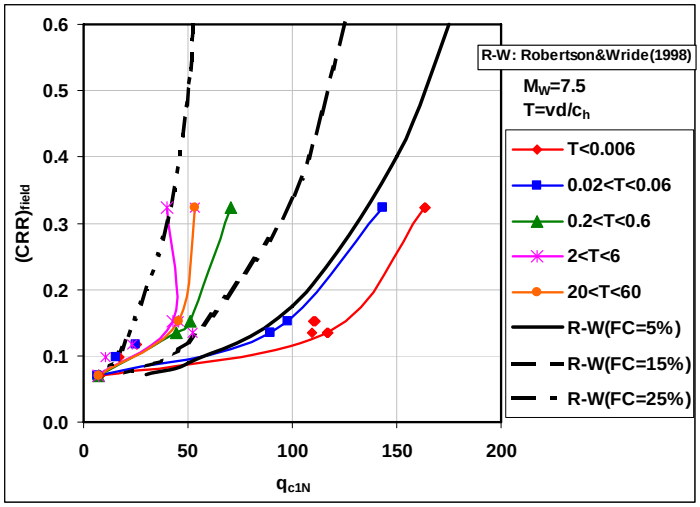

Fig. 7 $(CRR)_{field}$ versus q_{c1N}

Fig.7 shows the relationship for q_{c1N}-$(CRR)_{field-7.5}$. As T increases (which is attributed to increase in silt content and decrease in k and c_h) the CRR versus q_{c1N} curves shift to the left. With further increase in T, the curves merge together. Also shown in Fig.7 are the curves (denoted by R-W) recommended by Robertson and Wride (1997) corresponding to nearly clean sands, silty sands at nearly 15% silt content and 35% silt content, respectively. The curves corresponding to T<0.006 tend to follow the R-W curves for clean sands. The curves corresponding to 0.02<T<0.06 tend to follow the R-W curve for 15% silt content. The remaining curves tend to follow the R-W curve for 35% silt content. It appears from Fig.7 that the ranges of T greater than about 1 could be bundled together. The ranges of T values selected herein are to be considered tentative.

Although the T-dependent q_{c1N}-CRR relationships depict the same trend as observed in the field-based liquefaction screening procedures, additional numerical and physical simulation verification studies are needed to validate and refine this trend.

As part of this validation program three laminar box shaking tests have been completed. So far these shaking tests have been conducted in clean sand only. Tests involving silty sands have not been completed yet. The tests involved building a 16 ft high soil in a laminar box and shaking. These tests were instrumented with accelerometers and piezometers, among other sensors. Pre-shaking CPT penetration tests were also done. Detailed analyses of the experimental data are available in Ecemis (2007). The relationship between the liquefaction resistance and cone penetration resistance obtained from these tests are shown in Fig.8. The experimental data closely follows the lines corresponding to

clean sand. Experimental data on silty sands will be reported elsewhere when they become available.

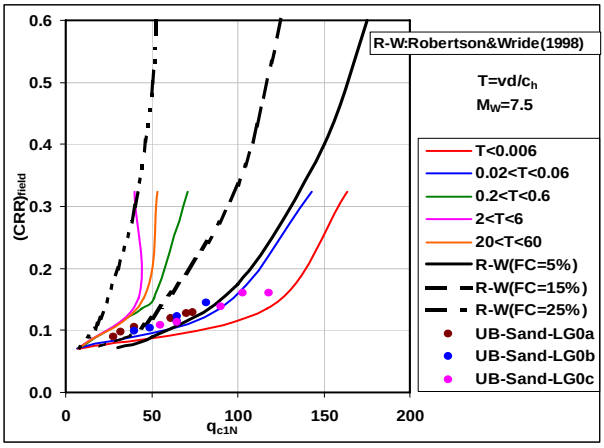

Fig.8 CRR_{field} versus q_{c1N}

4 CONCLUSIONS

Sands and silty sands with the same liquefaction resistance have significantly different hydraulic conductivity and coefficient of consolidation characteristics, due to significant differences in pore size distribution characteristics between sand and silty sands. Pore pressure response around the cone tip during penetration and normalized cone tip resistances are significantly different for sand and silty sand with similar or nearly the same equivalent relative density $(D_{rc})_{eq}$. For the same $(D_{rc})_{eq}$, q_{c1N} increases with a decrease in T (or increase in permeability). At large values of T the cone resistance represents an undrained cone resistance of the soil. At low T values the cone resistance is derived from a nearly drained response of a soil. It has been shown before that cyclic resistance is primarily governed by $(D_{rc})_{eq}$ irrespective of permeability of the soil. Relationship between liquefaction resistance (CRR at 15 cycles) and normalized cone penetration resistance q_{c1N} is dependent on the normalized cone penetration velocity T. A permeability and compressibility dependent liquefaction-screening chart based on normalized cone penetration resistance and T (=vd/c_h) is proposed. The proposed relationships are compared with the experimental results obtained from full-scale 1-g laminar box shake table liquefaction experiments and cone penetration tests on clean sands. Further assessment of this relationship using 1-g shake table testing on silty sands is currently underway.

Acknowledgement: Financial support for this work was provided by the USGS/NEHRP program. It is gratefully appreciated.

REFERENCES:

ABAQUS, 2000. User's manual, Hibbitt, Karlsson & Sorensen, Inc., Fremont, CA.

Aubeny, C. P., (1992). "Rational interpretation of in situ tests in cohesive soils", *PhD thesis, Dept. of Civil and Envir. Eng.*, MIT, Cambridge, Mass.

Andrus, R.D. and Stokoe, K.H. (2000) "Liquefaction resistance of soils from shear-wave velocity", *J. Geotech. and Geoenv. Eng., ASCE*, 2000; 126(11): 1015-25

Baligh M, and Levadoux, J., 1986. Consolidation after Undrained Piezocone Penetration. II: *Interpretation, J. Geotechnical Eng.*, 112(7), 727-745.

Carraro, J.A.H., Bandini, P., and Salgado, R. (2003) "Liquefaction resistance of clean and nonplastic silty sands based on cone penetration resistance", *J, Geotech. and Geoenv. Eng., ASCE*, 129(11), 965-976.

Castro, G. (1975) "Liquefaction and cyclic mobility of saturated sands", *J. Geotech. Eng. Div., ASCE*, 101(6), 551-569.

Ecemis, N. (2007). "Effects of soil permeability and compressibility on liquefaction screening using cone

penetration resistance", *PhD Dissertation, University at Buffalo*, Buffalo, NY, In preparation.

JGS, (1995) Remedial measures against soil liquefaction: *From investigation and design to implementation, Port and Harbor Research Inst*., Japan, 1995

Koester, J. P. (1994) "The influence of fines type and content on cyclic strength" *ASCE Geotech Spec*. Pub. 44, 17-33.

Mitchell, J.K, and Tseng, D-J. (1991) "Assessment of liquefaction potential by cone penetration resistance", *Proc., Seed memorial symp*., ed. M. Duncan, Berkeley, CA, 335-350.

Robertson, P.K. and Wride, C.E. (1997) "Evaluation of cyclic liquefaction potential based on the CPT", *Seis. Behavior of Ground & Geotech Struct., Balkema Publs*., 1997; 269-278.

Schnaid, F. (2005) "Geo-characterization and properties of natural soils bu insitu tests", *Proc. 16th Intl. Conf on Soil Mech. and Geotech. Eng.*, Osaka, Japan, Millpress, vol.1, 3-45.

Seed, H. B., Martin, G. R., and Pyke, C. K. (1978) "Effects of multi-directional shaking on pore pressure development in sands", *J. Geotech. Eng. Div., ASCE*, 104(1), 27-44.

Seed, H.B., Idriss, I.M, and Arango, I. (1983) "Evaluation of liquefaction potential using field performance data", *J. Geotech. Eng., ASCE*, 109(3): 458-482

Shenthan, T. (2001) "Factors affecting liquefaction mitigation in silty soils using stone columns", *MS Thesis, Univ. at Buffalo*, SUNY, NY, p129

Stokoe KH, II, Darendeli MB, Andrus RD, Brown LT. (1999) "Dynamic soil properties: laboratory, field and correlation studies", *2nd Intl. Conf. Earthq. Geotech. Eng., ed. P. Seco e Pinto*, vol.3, A.A.Balkema Press, 811-856.

TETC (1990) "Geotechnical investigation, Pier 300, 42-Acre Landfill ground modification project", *prepared by The Earth technology Corp. for Port of Los Angeles, California*.

Thevanayagam, S. (1999) "Liquefaction and shear wave velocity characteristics of silty/gravely soils – implications for bridge foundations", *Proc. 15th US-Japan Bridge Workshop, PWRI*, Japan, ed. Nishikawa, 1999; 133-147.

Thevanayagam, S. Martin, G.R, Shenthan, T. and Liang J. (2001) "Post-liquefaction pore pressure dissipation and densification in silty soils", *Proc., 4th Intl. Conf. Recent Adv. Geot. Earthq. Eng. & Soil Dyn.*, San Diego, ed. S. Prakash, 2001; Paper# 4.28.

Thevanayagam, S., Shenthan, T., Mohan, S. and Liang, J. (2002), "Undrained fragility of sands, silty sands and silt", *ASCE, J. Geotech. & Geoenv. Eng.*, 128 (10), 849-859.

Thevanayagam, S. and Martin, G. R. (2002) "Liquefaction in silty soils - screening and remediation issues", *Soil Dyn. and Earthq. Eng.*, 22, 1034-1042.

Thevanayagam, S., Shenthan, T., and Kanagalingam, T., (2003). "Role of intergranular contacts on mechanisms causing liquefaction and slope failures in silty sands" *Final Report, USGS Award No. 01HQGR0032 and 99HQGR0021; US Geological Survey, Department of Interior, USA*, http://erp-web.er.usgs.gov/reports/abstract/2001/pt/01hqgr0032-report.pdf, 396p.

Thevanayagam, S., N.Ecemis, T.Kanagalingam, and G.R.Martin, (2006) "Effects of Fines on Liquefaction Screening using Penetration Resistance" *8th U.S. National Conference on Earthquake Engineering*, San Francisco, CA, April

Thevanayagam, S. (2007) "Intergrain contact density indices for granular mixes –I: Framework", J. Earthquake engineering and engineering vibrations, June.

Thevanayagam, S. (2007) "Intergrain contact density indices for granular mixes –II: Liquefaction resistance", J. Earthquake engineering and engineering vibrations, June.

Vaid, Y. (1994), "Liquefaction of silty soils", *ASCE Geotech Spec*. Pub. 44, 1-16.

Youd TL, and Gilstrap SD. (1999) "Liquefaction and deformation of silty and fine-grained soils", *Proc., 2nd Intl. Conf. Earthquake Geotech. Eng., ed. P. Seco e Pinto*, vol.3, A.A.Balkema Press, 1013-1020.

Youd, T.L, and Idriss, I.M, (1997) Proc., NCEER workshop on Evaluation of liquefaction resistance of soils, *NCEER Tech. Report NCEER-97-0022*, 1997; 276p.

Zlatovic, S. and Ishihara, K. (1997) "Normalized behavior of very loose non-plastic soils: effects of fabric", *Soils and Foundations*, 37(4): 45-57.